Reaffirmation of Mechanistic Proteomic Signatures Accompanying SGLT2 Inhibition in Patients With Heart Failure: a Validation Cohort of the EMPEROR Program

Supplementary Appendix

Supplementary Methods 1.
Methodology of Sampling for Biobanking in the EMPEROR-Reduced and EMPEROR-Preserved Trials.

1. Organizational principles of sampling for biobanking in EMPEROR trials.

Participation in biobanking sampling (including DNA) was voluntary and not a prerequisite for trial participation. Biobanking samples were taken only after separate ICF had been given in accordance with local ethical and regulatory requirements. Measures were in place to comply with the rules for the collection, biobanking and future use of biological samples and clinical data, in particular

- Sample and data usage in accordance with the separate biobanking ICF.
- The BI-internal facilities storing biological samples from clinical trial participants as well as the external banking facility are qualified for the storage of biological samples.
- An appropriate sample and data management system, incl. audit trail for clinical data and samples to identify and destroy such samples according to ICF in place
- A fit for the purpose documentation required (biomarker proposal, analysis plan and report) to ensure compliant usage
- A fit for purpose approach for assay/equipment validation required depending on the intended use of the biomarker data
- Possibility of samples and/or data transfer to third parties and other countries is specified in the biobanking ICF

2. Countries participating in biobanking in EMPEROR trials

EMPEROR-Reduced	EMPEROR-Preserved
Argentina, Australia, Canada, Czech Republic, France, Germany, Hungary, India, Italy, Japan, Mexico, Netherlands, Poland, Republic of Korea, Spain, United Kingdom, United States	Argentina, Australia, Canada, Colombia, Czech Republic, Germany, Hungary, India, Italy, Japan, Mexico, Netherlands, Poland, Republic of Korea, Romania, Singapore, South Africa, Spain, United Kingdom, United States
Countries not participating in biobanking	
Belgium, Brazil, China	Belgium, Brazil, China

3. Timing and methodology of sampling

Sampling for Biobanking in EMPEROR-Reduced and EMPEROR-Preserved trials was performed at the following timepoints, specified by the clinical trial protocols:

DNA: preferably at visit 2 (randomization); plasma, serum and urine banking: visit 2 (randomization), visit 4 (week 12), visit 8 (week 52)

DNA banking: ≈8.5 mL blood were drawn into a PAXgene Blood DNA Tube

Plasma banking: ≈10 mL blood were drawn into an EDTA blood collection tube.

Serum banking: ≈8.5mL blood were drawn into a serum separation tube.

Urine banking: ≈10 mL urine (preferably morning mid-stream urine) were collected.

For all biological samples collected, detailed instructions on sampling, preparation, processing, shipment and storage were provided in the laboratory manual. Plasma, serum and urine samples have been being stored at an external biobanking facility contracted by the Sponsor; DNA, extracted from the original whole blood sample, has been being stored at the Sponsor.

Supplementary Methods 2.
Consort Diagram for Olink® Explore 3072 Measurements

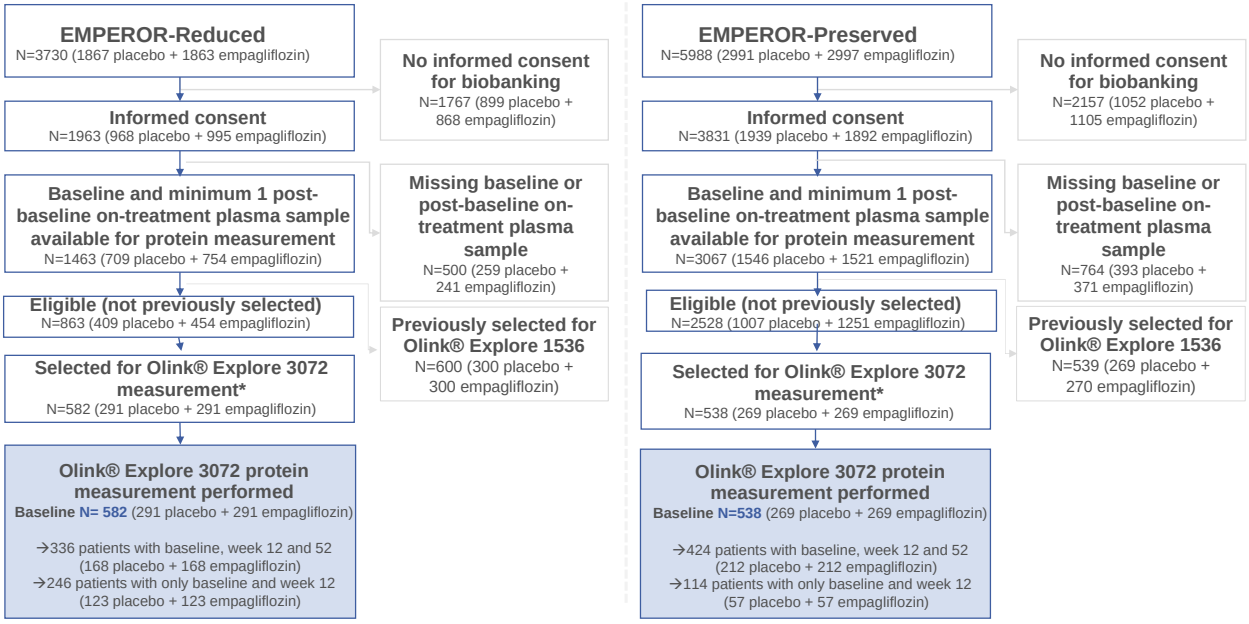

*Random sampling stratified by treatment and availability of data.

Supplementary Table S1.
Baseline Characteristics of Patients in Discovery Cohort 1 and in Validation Cohort 2 (EMPEROR-Reduced and EMPEROR-Preserved Combined)

	Discovery Cohort 1 Olink® Explore 1536 (n=1134)	**Validation Cohort 2** Olink® Explore 3072 (n=1120)	**P Value**
Age (years)	70.0 ± 10.0	70.2 ± 9.7	0.62
Women — number (%)	361 (31.8)	350 (31.3)	0.77
Race — number (%)			
White	958 (84.5)	956 (85.4)	0.92
Black	24 (2.1)	25 (2.2)	
Asian	96 (8.5)	88 (7.9)	
Other	45 (4.0)	41 (3.7)	
Region — number (%)			
North America	154 (13.6)	119 (10.6)	0.11
Latin America	217 (19.1)	210 (18.8)	
Europe	642 (56.6)	686 (61.3)	
Asia	86 (7.6)	79 (7.1)	
Other	35 (3.1)	26 (2.3)	
NYHA functional classification — number (%)			
Class I	0	1 (0.1)	0.61
Class II	910 (80.2)	884 (78.9)	
Class III	221 (19.5)	233 (20.8)	
Class IV	3 (0.3)	2 (0.2)	
Body mass index (kg/m^2)	29.3 ± 5.6	29.6 ± 5.5	0.36
Heart rate (beats/min)	70.5 ± 11.8	70.8 ± 12.0	0.48
Systolic blood pressure (mmHg)	128.0 ± 15.7	128.5 ± 16.2	0.47
Left ventricular ejection fraction (%)	40.1 ± 15.0	40.1 ± 14.9	1.00
Median NT-proBNP (IQR), pg/mL	1383 (710, 2483)	1331 (713, 2461)	0.51
Etiology of heart failure — number (%)			
Ischemic	506 (44.6)	540 (48.2)	0.09
Nonischemic	628 (55.4)	580 (51.8)	
Cardiovascular history — number (%)			
Hospitalization for heart failure within 12 months	299 (26.4)	301 (26.9)	0.79
Atrial fibrillation	530 (46.7)	519 (46.3)	0.79
Diabetes mellitus	548 (48.3)	568 (50.7)	0.26
Hypertension	941 (83.0)	949 (84.7)	0.26
Estimated glomerular filtration rate (eGFR)			
Mean (mL/min/1.73 m^2)	60.5 ± 20.4	61.6 ± 19.8	0.20
Number (%) with eGFR <60 mL/min/1.73 m^2	579 (51.1)	540 (48.2)	0.18

Plus-minus values are means ± SD. Race was self-reported; patients who identified with >1 race or with no race were classified as other. The body-mass index is the weight in kilograms divided by the square of the height in meters. Atrial fibrillation refers to any reports from any ECG before treatment intake or history of atrial fibrillation reported in medical history. eGFR was calculated based on data from subjects with valid eGFR measurements. For NTproBNP based on log−transformed results. P values based on t−test for continuous variables and chi−square test for categorical variables. Abbreviations: NYHA, New York Heart Association; NT-proBNP, N-terminal pro brain natriuretic peptide; IQR, interquartile range; eGFR, estimated glomerular filtration rate.

Supplementary Table S2.
Listing of 117 Proteins With ≥10% Between-Group Difference With FDRq<1%, Adjusted for Change in eGFR, in Validation Cohort 2

Protein	Uniprot ID	Emplagliflozin vs placebo [log_2 fold change]	95% CI lower bound	95% CI higher bound	FDRq
Alpha-synuclein	P37840	0.4497	0.2140	0.6853	0.20%
ATPase inhibitor, mitochondrial	Q9UII2	0.3093	0.1266	0.4920	0.60%
Retinol-binding protein 2	P50120	0.2997	0.2085	0.3908	<0.01%
IST homolog associated with ESCRT-III	P53990	0.2808	0.1119	0.4497	0.70%
Tubulin-specific chaperone A	O75347	0.2697	0.1152	0.4242	0.47%
DnaJ homolog subfamily C member 9	Q8WXX5	0.2585	0.1065	0.4105	0.58%
Cystatin-SN	P01037	0.2584	0.1589	0.3578	<0.01%
DnaJ homolog subfamily B member 1	P25685	0.2562	0.0952	0.4171	0.98%
C-C motif chemokine 5	P13501	0.2541	0.0972	0.4111	0.85%
Fatty acid-binding protein, liver	P07148	0.2496	0.1368	0.3623	0.03%
Creatine kinase U-type, mitochondrial	P12532	0.2490	0.1237	0.3744	0.13%
Uncharacterized protein C9orf40	Q8IXQ3	0.2421	0.1070	0.3773	0.38%
Ubiquitin thioesterase OTU1	Q5VVQ6	0.2399	0.1156	0.3642	0.18%
C-C motif chemokine 28	Q9NRJ3	0.2344	0.1416	0.3272	<0.01%
Chromogranin-A	P10645	0.2307	0.1255	0.3358	0.04%
Acylphosphatase-1	P07311	0.2304	0.1126	0.3483	0.17%
Hsc70-interacting protein	P50502	0.2301	0.1107	0.3495	0.19%
Fatty acid-binding protein, heart	P05413	0.2278	0.1467	0.3088	<0.01%
Fatty acid-binding protein 5	Q01469	0.2267	0.1225	0.3309	0.04%
Insulin-like growth factor-binding protein 1	P08833	0.2213	0.0851	0.3575	0.83%
Carbonic anhydrase 2	P00918	0.2204	0.0891	0.3516	0.65%
Immunoglobulin-binding protein 1	P78318	0.2202	0.0968	0.3436	0.39%
Transferrin receptor protein 1	P02786	0.2195	0.1595	0.2795	<0.01%
Myeloid-derived growth factor	Q969H8	0.2167	0.0861	0.3473	0.71%
Erythroid membrane-associated protein	Q96PL5	0.2126	0.1492	0.2761	<0.01%
Erythropoietin	P01588	0.2099	0.0945	0.3253	0.33%
Uroporphyrinogen decarboxylase	P06132	0.2085	0.0800	0.3369	0.84%
Gastrotropin	P51161	0.2065	0.1201	0.2928	0.01%
BolA-like protein 2	Q9H3K6	0.2015	0.0928	0.3102	0.27%
Oncostatin-M	P13725	0.2004	0.0827	0.3182	0.58%
UBX domain-containing protein 1	Q04323	0.2004	0.0789	0.3220	0.75%
Thymosin beta-10	P63313	0.1983	0.0844	0.3122	0.48%
Osteocalcin	P02818	0.1978	0.0899	0.3057	0.30%
Serine protease inhibitor Kazal-type 4	O60575	0.1977	0.1325	0.2629	<0.01%
Anaphase-promoting complex subunit CDC26	Q8NHZ8	0.1967	0.0996	0.2938	0.11%
Appetite-regulating hormone	Q9UBU3	0.1966	0.1062	0.2869	0.04%
Carcinoembryonic antigen-related cell adhesion molecule 8	P31997	0.1936	0.1016	0.2855	0.06%
C-X-C motif chemokine 6	P80162	0.1909	0.0834	0.2984	0.40%
Pepsin A-4	P0DJD7	0.1882	0.1039	0.2724	0.03%
DnaJ homolog subfamily B member 2	P25686	0.1878	0.0793	0.2964	0.50%
DnaJ homolog subfamily A member 4	Q8WW22	0.1877	0.0820	0.2935	0.40%
Uromodulin	P07911	0.1877	0.1385	0.2369	<0.01%
Putative peptidyl-tRNA hydrolase PTRHD1	Q6GMV3	0.1873	0.0739	0.3008	0.73%
AMP deaminase 3	Q01432	0.1823	0.0774	0.2873	0.48%

Trefoil factor 1	P04155	0.1821	0.1107	0.2536	<0.01%
Sorting nexin-15	Q9NRS6	0.1810	0.0856	0.2763	0.21%
Programmed cell death protein 5	O14737	0.1807	0.0872	0.2742	0.18%
Cell surface A33 antigen	Q99795	0.1806	0.0709	0.2904	0.76%
Ribonuclease 4	P34096	0.1805	0.1186	0.2423	<0.01%
Beta-crystallin B1	P53674	0.1741	0.0865	0.2617	0.13%
Dual specificity mitogen-activated protein kinase kinase 1	Q02750	0.1738	0.0812	0.2665	0.24%
Bone marrow proteoglycan	P13727	0.1718	0.1097	0.2339	<0.01%
Proteinase-activated receptor 1	P25116	0.1716	0.0807	0.2625	0.23%
Kynurenine--oxoglutarate transaminase 1	Q16773	0.1708	0.0633	0.2782	0.99%
Ficolin-1	O00602	0.1696	0.0897	0.2495	0.06%
Promotilin	P12872	0.1695	0.0880	0.2510	0.07%
Mitochondrial import receptor subunit TOM20 homolog	Q15388	0.1694	0.0631	0.2757	0.97%
Nucleosome assembly protein 1-like 4	Q99733	0.1686	0.0720	0.2653	0.47%
Acyl-CoA-binding protein	P07108	0.1674	0.0729	0.2619	0.41%
Serine protease inhibitor Kazal-type 1	P00995	0.1664	0.1167	0.2161	<0.01%
Lithostathine-1-alpha	P05451	0.1660	0.0925	0.2395	0.02%
NADH dehydrogenase [ubiquinone] iron-sulfur protein 6, mitochondrial	O75380	0.1659	0.0656	0.2663	0.73%
Regenerating islet-derived protein 3-alpha	Q06141	0.1655	0.0965	0.2345	0.01%
V-set and immunoglobulin domain-containing protein 2	Q96IQ7	0.1653	0.0971	0.2335	0.01%
Retinoid-binding protein 7	Q96R05	0.1649	0.0829	0.2469	0.12%
Dickkopf-related protein 4	Q9UBT3	0.1646	0.0989	0.2303	<0.01%
Complement factor H-related protein 5	Q9BXR6	0.1644	0.0946	0.2342	0.01%
Matrix metalloproteinase-9	P14780	0.1643	0.0706	0.2579	0.45%
Renin	P00797	0.1642	0.0748	0.2537	0.30%
2'-deoxynucleoside 5'-phosphate N-hydrolase 1	O43598	0.1622	0.0629	0.2614	0.80%
TP53-regulated inhibitor of apoptosis 1	O43715	0.1616	0.0707	0.2526	0.40%
Protein S100-G	P29377	0.1611	0.0948	0.2274	0.01%
Serine protease inhibitor Kazal-type 2	P20155	0.1608	0.1050	0.2165	<0.01%
Fatty acid-binding protein, adipocyte	P15090	0.1597	0.0908	0.2286	0.02%
Midkine	P21741	0.1594	0.0917	0.2271	0.01%
Phosphatidylethanolamine-binding protein 1	P30086	0.1593	0.0664	0.2522	0.54%
Stanniocalcin-1	P52823	0.1586	0.0924	0.2248	0.01%
C-C motif chemokine 7	P80098	0.1584	0.0897	0.2270	0.02%
Guanylin	Q02747	0.1576	0.0978	0.2173	<0.01%
Protein phosphatase 1 regulatory subunit 14A	Q96A00	0.1575	0.0601	0.2548	0.86%
Copper transport protein ATOX1	O00244	0.1570	0.0693	0.2447	0.38%
Pappalysin-1	Q13219	0.1559	0.0598	0.2521	0.84%
Galectin-4	P56470	0.1557	0.0882	0.2232	0.02%
Protein FAM3D	Q96BQ1	0.1555	0.0870	0.2240	0.02%
Lymphocyte antigen 6D	Q14210	0.1551	0.1030	0.2072	<0.01%
OTU domain-containing protein 7B	Q6GQQ9	0.1541	0.0682	0.2399	0.37%
Stromal cell-derived factor 1	P48061	0.1540	0.0951	0.2128	<0.01%
Ubiquitin/ISG15-conjugating enzyme E2 L6	O14933	0.1535	0.0575	0.2495	0.95%
26S proteasome non-ATPase regulatory subunit 9	O00233	0.1532	0.0585	0.2479	0.86%
Angiopoietin-related protein 4	Q9BY76	0.1502	0.0905	0.2099	<0.01%
Epithelial cell adhesion molecule	P16422	0.1497	0.0694	0.2300	0.26%
Tumor necrosis factor ligand superfamily member 14	O43557	0.1491	0.0601	0.2381	0.66%

Ribonuclease K6	Q93091	0.1490	0.0940	0.2040	<0.01%
Kunitz-type protease inhibitor 3	P49223	0.1489	0.0711	0.2267	0.20%
Proteoglycan 3	Q9Y2Y8	0.1485	0.0918	0.2051	<0.01%
Calcitonin	P01258	0.1480	0.0776	0.2183	0.06%
Leukocyte cell-derived chemotaxin-2	O14960	0.1479	0.0745	0.2213	0.12%
Elafin	P19957	0.1477	0.0842	0.2113	0.02%
Proactivator polypeptide-like 1	Q6NUJ1	0.1464	0.0928	0.2000	<0.01%
Prorelaxin H2	P04090	0.1462	0.0814	0.2110	0.02%
C-C motif chemokine 22	O00626	0.1458	0.0587	0.2329	0.66%
Cadherin EGF LAG seven-pass G-type receptor 2	Q9HCU4	0.1452	0.0950	0.1955	<0.01%
Hydroxysteroid dehydrogenase-like protein 2	Q6YN16	0.1432	0.0671	0.2194	0.23%
Intercellular adhesion molecule 4	Q14773	0.1430	0.0962	0.1898	<0.01%
Secreted Ly-6/uPAR-related protein 1	P55000	0.1428	0.0919	0.1936	<0.01%
Proenkephalin-A	P01210	0.1427	0.0920	0.1934	<0.01%
NADH-cytochrome b5 reductase 2	Q6BCY4	0.1418	0.0684	0.2153	0.18%
Glycosylphosphatidylinositol-anchored high density lipoprotein-binding protein 1	Q8IV16	0.1415	0.0621	0.2209	0.39%
Junctional adhesion molecule C	Q9BX67	0.1413	0.0733	0.2094	0.07%
Protein GPR15L	Q6UWK7	0.1413	0.0608	0.2218	0.45%
Insulin-like growth factor-binding protein 4	P22692	0.1412	0.0780	0.2043	0.03%
Trefoil factor 2	Q03403	0.1412	0.0743	0.2080	0.06%
Cerebral dopamine neurotrophic factor	Q49AH0	0.1399	0.0936	0.1862	<0.01%
Ganglioside GM2 activator	P17900	0.1395	0.0833	0.1957	0.01%
Retinoid-inducible serine carboxypeptidase	Q9HB40	0.1390	0.0557	0.2223	0.68%
C-C motif chemokine 18	P55774	0.1389	0.0616	0.2162	0.37%

Supplementary Table S3.
Biological Actions of 58 Proteins With ≥10% But <15% Between-Group Difference and FDRq<1% (Adjusted for Change in eGFR) and With Effects on the Heart or Kidneys (Validation Cohort 2)

Protein	Uniprot ID	Empagliflozin vs placebo [log_2 fold change (95%CI)]	False discovery rate (%)	Biological Functions on the Heart and Kidney
BolA-like protein 2 (BOLA2)	Q9H3K6	0.20 (0.09-0.31)	0.27%	Promotes iron-sulfur protein maturation, enhancing uptake and inhibiting storage of iron
Oncostatin-M (OSM)	P13725	0.20 (0.08-0.32)	0.58%	Effects depending on duration of upregulation. Can promote cardiac regeneration and vasculogenesis, leading to improved function
UBX (ubiquitin) domain-containing protein 1 (UBXN1)	Q04323	0.20 (0.08-0.32)	0.75%	Essential for endolysosomal sorting critical for autophagosome maturation and autophagic flux; mutes proinflammatory signaling
Thymosin beta-10 (TMSB10)	P63313	0.20 (0.08-0.31)	0.48%	Regeneration and restoration of renal tubular epithelial cellular architecture
Osteocalcin (BGLAP)	P02818	0.20 (0.09-0.31)	0.30%	Facilitates fatty acid metabolism and ATP generation for myofiber contraction
Anaphase-promoting complex subunit CDC26 (APC/C)	Q8NHZ8	0.20 (0.10-0.29)	0.11%	Pivotal link in autophagic control of runaway meiotic divisions; antagonist of cellular aging
Ghrelin (GHRL)	Q9UBU3	0.20 (0.11-0.29)	0.04%	Promotes autophagic flux to inhibit post-injury cardiac hypertrophy and fibrosis
DnaJ homolog subfamily B member 2 (DNAJB2)	P25686	0.19 (0.08-0.30)	0.50%	Positioned to facilitate chaperone-mediated protein folding and autophagy
DnaJ homolog subfamily A member 4 (DNAJA4)	Q8WW22	0.19 (0.08-0.290	0.40%	Positioned to facilitate chaperone-mediated protein folding and autophagy
Uromodulin (UMOD)	P07911	0.19 (0.14-0.24)	0.01%	Counter-regulatory enhanced renal tubular sodium reabsorption
Adenosine monophosphate deaminase 3 (AMPD3)	Q01432	0.18 (0.07-0.29)	0.48%	Increases cardiac branched-chain amino acid metabolism, yielding ATP needed for myofiber contraction
Trefoil factor 1 (TFF1)	P04155	0.18 (0.11-0.25)	< 0.01%	Regeneration and restoration of renal tubular epithelial cellular architecture
Sorting nexin-15 (SNX15)	Q9NRS6	0.18 (0.09-0.27)	0.21%	Mediates intracellular trafficking and autophagic clearance of proteins, e.g., resulting in decreased insulin signaling
Programmed cell death protein 5 (PDCD5)	O14737	0.18 (0.08-0.27)	0.18%	Promotes autophagy to negatively regulate cardiac remodeling
Dual specificity mitogen-activated protein kinase kinase 1 (MAP2K1, MEK)	Q02750	0.17 (0.08-0.27)	0.24%	Member of mitogen activated kinase family involved in promotion of autophagy
Proteinase-activated receptor 1 (PAR1)	P25116	0.17 (0.08-0.26)	0.23%	Promotes cardiomyocyte hypertrophy and fibroblast proliferation
Kynurenine--oxoglutarate transaminase 1 (KYAT1)	Q16773	0.17 (0.06-0.28)	0.99%	Promote formation of kynurenic acid, a glutamate antagonist and sympatholytic
Mitochondrial import receptor subunit TOM20 homolog (TOMM20)	Q15388	0.17 (0.06-0.28)	0.97%	Facilitates transport of proteins into the mitochondria to facilitate ATP production; used as a marker of mitophagy

Nucleosome assembly protein 1-like 4 (NAP1L4)	Q99733	0.17 (0.07-0.27)	0.47%	Histone chaperone that can promote cardiac fibrosis and impairs cardiac function
Acyl-CoA-binding protein (ACBP1)	P07108	0.17 (0.07-0.26)	0.41%	Circulating biomarker of enhanced intracellular autophagic flux
Lithostathine-1-alpha (REG1A)	P05451	0.17 (0.09-0.24)	0.02%	Role in tissue regeneration; upregulated in the heart following acute injury
NADH dehydrogenase [ubiquinone] iron-sulfur protein 6, mitochondrial (NDUFS6)	O75380	0.17 (0.07-0.27)	0.73%	Iron-sulfur protein that promotes mitochondrial oxidative phosphorylation and ATP production; deficiency causes cardiomyopathy
Retinoid-binding protein 7 (RBP7)	Q96R05	0.16 (0.08-0.25)	0.12%	Member of fatty-acid binding protein family, promoting anti-oxidant activity of vascular endothelium
Complement factor H-related protein 5 (CFHR5)	Q9BXR6	0.16 (0.09-0.23)	0.01%	Recruited into tissues injured by inflammation, associated with chronic kidney disease
Matrix metalloproteinase-9 (MMP9)	P14780	0.16 (0.07-0.25)	0.45%	Driver of extracellular matrix degradation; intracellular MMP9 promotes autophagic flux and differentiation of cardiac stem cells
Renin	P00797	0.16 (0.07-0.25)	0.30%	Counter-regulatory enhanced renal tubular sodium reabsorption
TP53-regulated inhibitor of apoptosis 1 (TRIAP1)	O43715	0.16 (0.07-0.25)	0.40%	Mediates phospholipid transfer into mitochondria; mitigates development of podocyte apoptosis
Protein S100-G (S100G)	P29377	0.16 (0.09-0.23)	0.01%	Also known as calbindin-D28k, it mediates calcium transport in distal tubules
Adipocyte fatty acid-binding protein (A-FABP, FABP4)	P15090	0.16 (0.09-0.23)	0.02%	Secreted as a result of increased sirtuin-1 signalling and acts as a blood-borne indicator of autophagic flux
Midkine (MDK)	P21741	0.16 (0.09-0.23)	0.01%	Context-dependent promotion and attenuation of cardiac remodelling; upregulates autophagy in the heart
Phosphatidylethanolamine-binding protein 1 (PEBP1, RKIP)	P30086	0.16 (0.07-0.25)	0.54%	Scaffolding protein that induces ferroptosis; acts on calcium transients to sensitize heart to effects of catecholamines and angiotensin
Stanniocalcin-1 (STC1)	P52823	0.16 (0.09-0.22)	0.01%	Cardioprotective by regulating cardiac calcium currents to prevent calcium overload. Promotes calcium transport in renal tubules
Guanylin (GUCA2A)	Q02747	0.16 (0.10-0.22)	< 0.01%	Promotes natriuresis by inhibiting proximal tubular sodium-hydrogen exchanger 3
Protein phosphatase 1 regulatory subunit 14A (PPP1R14A)	Q96A00	0.16 (0.06-0.25)	0.86%	Inhibits myosin phosphatase, leading to myocyte calcium sensitization
Copper transport protein antioxidant 1 (ATOX1)	O00244	0.16 (0.07-0.24)	0.38%	Copper-dependent transcription factor; suppression leads to oxidative stress and cardiac dysfunction
Pappalysin-1 (PAPP-A)	Q13219	0.16 (0.06-0.25)	0.84%	Releases insulin-like growth factor 1 from binding, thus promoting chronic kidney disease
Galectin-4 (LGALS4)	P56470	0.16 (0.09-0.22)	0.02%	Promotes transcytosis of transferrin receptor, preventing its degradation
FAM3 metabolism regulating signaling molecule D (FAM3D)	Q96BQ1	0.16 (0.09-0.22)	0.02%	Reduces injury and inflammation, and enhances recovery of cardiac function after ischemia
OTU domain-containing protein 7B (OTUD7B)	Q6GQQ9	0.15 (0.07-0.24)	0.37%	OTUD-7B deubiquitination suppresses Akt-mTOR thereby enhancing autophagy, and attenuates pathological cardiac hypertrophy

Stromal cell-derived factor 1 (SDF-1)	P48061	0.15 (0.10-0.21)	< 0.01%	Attenuates cardiomyocyte apoptosis and mutes development of cardiomyopathy; promotes stem cell migration and angiogenesis
Ubiquitin/ISG15-conjugating enzyme E2 L6 (UBE2L6)	O14933	0.15 (0.06-0.25)	0.95%	E2 ubiquitin-conjugating enzyme that modulates autophagic flux
26S proteasome non-ATPase regulatory subunit 9 (PSMD9)	O00233	0.15 (0.06-0.25)	0.86%	Interplay of 26S proteosome ubiquination and autophagy are responsible for protein quality control
Angiopoietin-related protein 4 (ANGPTL4)	Q9BY76	0.15 (0.09-0.21)	< 0.01	Reduction of oxidative stress and endothelial cell injury by promoting autophagy
Epithelial cell adhesion molecule (EpCAM)	P16422	0.15 (0.07-0.23)	0.26%	Promotes adhesion, polarity and architecture. of renal tubular cells. Is enhanced during renal tubular regeneration
Tumor necrosis factor ligand superfamily member 14 (TNFSF14, LIGHT)	O43557	0.15 (0.06-0.24)	0.66%	Enhances cardiac and renal fibrosis, but can attenuate kidney injury by suppressing mitochondrial apoptosis
Calcitonin (alpha-type GCRP)	P01258	0.15 (0.08-0.22)	0.06%	Positive inotropic and systemic vasodilator effects; decreased calcium reabsorption in distal nephron
Elafin	P19957	0.15 (0.08-0.21)	0.02%	Protects against myocardial inflammation and injury, improving cardiac function
Prorelaxin H2 (RLN2)	P04090	0.15 (0.08-0.21)	0.02%	Systemic vasodilator and positive inotropic effects in heart; antifibrotic effects in kidney
Cadherin EGF LAG seven-pass G-type receptor 2 (CELSR2)	Q9HCU4	0.15 (0.10-0.20)	< 0.01%	Critical to epithelial cell polarity and restoration of renal tubular architecture
Intercellular adhesion molecule 4 (ICAM4)	Q14773	0.14 (0.10-0.19)	< 0.01%	Regulates contact among maturing erythroblasts to promote formation of erythropoietic islands
Secreted Ly-6/uPAR-related protein 1 (SLURP1)	P55000	0.14 (0.09-0.19)	< 0.01%	Prodifferentiation factor that stabilizes epithelial cell junctions; anti-inflammatory effects on endothelial cells
Proenkephalin-A (PENK-A)	P01210	0.14 (0.09-0.19)	< 0.01%	Surrogate for tissue opioid activation; controls calcium entry to exert cardioprotective effects; functions as a brake on kidney regeneration
NADH-cytochrome b5 reductase 2 (CYB5R2)	Q6BCY4	0.14 (0.07-0;.22)	0.18%	Catalyzes removal of iron from heme; promotes iron-mediated cell death (ferroptosis)
Junctional adhesion molecule C (JAM-C)	Q9BX67	0.14 (0.07-0.21)	0.07%	Maintains microenvironment for hematopoietic stem cells in the bone marrow; promotes angiogenesis
Insulin-like growth factor-binding protein 4 (IGFBP4)	P22692	0.14 (0.08-0.20)	0.03%	Cardioprotection through suppression of oxidative stress. Promotes cardiomyocyte induction from pluripotential stem cells
Cerebral dopamine neurotrophic factor (CDNF)	Q49AH0	0.14 (0.09-0.19)	<0.01%	Restores calcium transient and mitigates apoptosis in cardiomyocytes
Ganglioside GM2 activator (GM2A)	P17900	0.14 (0.08-0.20)	0.01%	Modulates proton pump of intercalated cells of renal collecting duct
Retinoid-inducible serine carboxypeptidase (SCPEP1, RISC)	Q9HB40	0.14 (0.06-0.22)	0.68%	Mediates retinoic acid-mediated anti-inflammatory effects; contributes to lysosome-mediated degradation and autophagy in vasculature and proximal renal tubule

REFERENCES FOR TABLE S3

BOLA2
Li H, Outten CE. Monothiol CGFS glutaredoxins and BolA-like proteins: [2Fe-2S] binding partners in iron homeostasis. Biochemistry. 2012;51:4377-89.

OSM
Ikeda S, Sato K, Takeda M, et al. Oncostatin M mediates cardioprotection via angiogenesis in ischemic heart disease. Am Heart J Plus. 2023 Oct 6;35:100331. doi: 10.1016/j.ahjo.2023.100331.

UBXN1
Trusch F, Matena A, Vuk M, et al. The N-terminal region of the Ubiquitin Regulatory X (UBX) domain-containing protein 1 (UBXD1) modulates interdomain communication within the Valosin-containing protein p97. J Biol Chem. 2015;290:29414-27.

TMSB10
Gerosa C, Fanni D, Nemolato S, et al Thymosin beta-10 expression in developing human kidney. J Matern Fetal Neonatal Med. 2010;23 Suppl 3:125-8.

APC/C
Wang F, Denic V, Lacefield S. Autophagy prevents runaway meiotic divisions. Autophagy. 2020;16:969-970.

Ghrelin
Liu H, Lv W, Ouyang L, Xu L. Ghrelin alleviates hypoxia/reoxygenation-induced H9C2 injury by activating autophagy and AMPK/ULK1 pathway. Cell Mol Biol (Noisy-le-grand). 2023;69:139-245.

DNAJB2
Claeys KG, Sozanska M, Martin JJ, et al. DNAJB2 expression in normal and diseased human and mouse skeletal muscle. Am J Pathol. 2010;176:2901-10.

DNAJA4
Abdul KM, Terada K, Gotoh T, Hafizur RM, Mori M. Characterization and functional analysis of a heart-enriched DnaJ/ Hsp40 homolog dj4/DjA4. Cell Stress Chaperones. 2002;7:156-66.

Uromodulin
Bachmann S. A novel role for Tamm-Horsfall protein (uromodulin) in the renal tubule. Kidney Int. 2018;94:652-655.

AMPD3
Ogawa T, Kouzu H, Osanami A, et al. Downregulation of extramitochondrial BCKDH and its uncoupling from AMP deaminase in type 2 diabetic OLETF rat hearts. Physiol Rep. 2023 Feb;11(4):e15608. doi: 10.14814/phy2.15608.

TFF1
Nieskens TTG, Persson M, Kelly EJ, Sjögren AK. A multicompartment human kidney proximal tubule-on-a-chip replicates cell polarization-dependent cisplatin toxicity. Drug Metab Dispos. 2020;48:1303-1311.

SNX15
Phillips SA, Barr VA, Haft DH, Taylor SI, Haft CR. Identification and characterization of SNX15, a novel sorting nexin involved in protein trafficking. J Biol Chem. 2001;276:5074-84.

PDCD5
Zhang S, Li G, Fu X, et al. PDCD5 protects against cardiac remodeling by regulating autophagy and apoptosis. Biochem Biophys Res Commun. 2015;461:321-8.

MAP2K1
Deng X, Yang Z, Li T, et al. Identification of 4 autophagy-related genes in heart failure by bioinformatics analysis and machine learning. Front Cardiovasc Med. 2024 Jan 29;11:1247079. doi: 10.3389/fcvm.2024.1247079.

PAR1
Fletcher EK, Ngwenyama N, Nguyen N, et al. Suppression of heart failure with PAR1 pepducin technology in a pressure overload model in mice. Circ Heart Fail. 2023;16(10):e010621 doi: 10.1161/CIRCHEARTFAILURE.123.010621.

KYAT1
Vayssettes-Courchay C, Bouysset F, Verbeuren TJ, Laubie M. Evidence against the involvement of the nucleus tractus solitarii in the sympatholytic effect of 8-hydroxy-2-(di-n-propylamino)tetralin in the cat. Eur J Pharmacol. 1995;285:299-304.

TOMM20
Zheng T, Waqng -Y, Chen Y, et al. Src activation aggravates podocyte injury in diabetic nephropathy via suppression of FUNDC1-mediated mitophagy. Front Pharmacol. 2022 May 9;13:897046. doi: 10.3389/fphar.2022.897046.

NAP1L4
Li T, Niu Z, Yu T, et al. Nucleosome assembly protein 1 like 1 (NAP1L1) promotes cardiac fibrosis by inhibiting YAP1 ubiquitination and degradation. MedComm (2020). 2023 Aug 15;4(5):e348. doi: 10.1002/mco2.348.

ACBP1
Abdellatif M, Montégut L, Kroemer G. Actionable autophagy checkpoints in cardiovascular ageing. Eur Heart J. 2023;44:4819-4821.

REG1A
Kiji T, Dohi Y, Takasawa S, Okamoto H, Nonomura A, Taniguchi S. Activation of regenerating gene Reg in rat and human hearts in response to acute stress. Am J Physiol Heart Circ Physiol. 2005;289:H277-84.

NDUFS6
Ke BX, Pepe S, Grubb DR, et al. Tissue-specific splicing of an Ndufs6 gene-trap insertion generates a mitochondrial complex I deficiency-specific cardiomyopathy. Proc Natl Acad Sci U S A. 2012;109:6165-70.

RBP7
Hu C, Keen HL, Lu KT, et al. Retinol-binding protein 7 is an endothelium-specific PPARgamma cofactor mediating an antioxidant response through adiponectin. JCI Insight. 2017 Mar 23;2(6):e91738. doi: 10.1172/jci.insight.91738.

CFHR5
Papp A, Papp K, Uzonyi B, et al. Complement factor H-related proteins FHR1 and FHR5 interact with extracellular matrix ligands, reduce factor h regulatory activity and enhance complement activation. Front Immunol. 2022 Mar 22;13:845953. doi: 10.3389/fimmu.2022.845953.

MMP9
Yadav SK, Mishra PK. Intracellular matrix metalloproteinase-9 mediates epigenetic modifications and autophagy to regulate differentiation in human cardiac stem cells. Stem Cells. 2021;39:497-506.

TRIAP1
Zhang SZ, Qiu XJ, Dong SS, et al. MicroRNA-770-5p is involved in the development of diabetic nephropathy through regulating podocyte apoptosis by targeting TP53 regulated inhibitor of apoptosis 1. Eur Rev Med Pharmacol Sci. 2019;23(3):1248-1256.

Potting C, Tatsuta T, König T, et al. TRIAP1/PRELI complexes prevent apoptosis by mediating intramitochondrial transport of phosphatidic acid. Cell Metab. 2013;18:287-95.

S100G
Lee CT, Ng HY, Lee YT, Lai LW, Lien YH. The role of calbindin-D28k on renal calcium and magnesium handling during treatment with loop and thiazide diuretics. Am J Physiol Renal Physiol. 2016;310:F230-6.

A-FABP/FABP4
Josephrajan A, Hertzel AV, Bohm EK, et al Unconventional secretion of adipocyte fatty acid binding protein 4 is mediated by autophagic proteins in a sirtuin-1-dependent manner. Diabetes. 2019;68:1767-1777.

Midkine
Sumida A, Horiba M, Ishiguro H, et al Midkine gene transfer after myocardial infarction in rats prevents remodelling and ameliorates cardiac dysfunction. Cardiovasc Res. 2010;86:113-21.

Shi Y, Ge J, Li R, Li Y, Lin L. Targeting of midkine alleviates cardiac hypertrophy via attenuation of oxidative stress and autophagy. Peptides. 2022 Jul;153:170800. doi: 10.1016/j.peptides.2022.170800.

Netsu S, Shishido T, Kitahara T, et al. Midkine exacerbates pressure overload-induced cardiac remodeling. Biochem Biophys Res Commun. 2014;443:205-10.

PEBP1/RKIP

Schmid E, Neef S, Berlin C, et al. Cardiac RKIP induces a beneficial β-adrenoceptor-dependent positive inotropy. Nat Med. 2015;21:1298-306.

Wolf S, Abd Alla J, Quitterer U. Sensitization of the angiotensin II AT1 receptor contributes to RKIP-induced symptoms of heart failure. Front Med (Lausanne). 2019 Jan 9;5:359. doi: 10.3389/fmed.2018.00359.

Wenzel SE, Tyurina YY, Zhao J, et al. PEBP1 wardens ferroptosis by enabling lipoxygenase generation of lipid death signals. Cell. 2017;171:628-641.e26.

Stanniocalcin-1 (STC1)

Liu D, Huang L, Wang Y, et al. Human stanniocalcin-1 suppresses angiotensin II-induced superoxide generation in cardiomyocytes through UCP3-mediated anti-oxidant pathway. PLoS One. 2012;7(5):e36994. doi: 10.1371/journal.pone.0036994.

Ellard JP, McCudden CR, Tanega C, et al. The respiratory effects of stanniocalcin-1 (STC-1) on intact mitochondria and cells: STC-1 uncouples oxidative phosphorylation and its actions are modulated by nucleotide triphosphates. Mol Cell Endocrinol. 2007;264:90-101.

Sheikh-Hamad D, Bick R, Wu GY, et al. Stanniocalcin-1 is a naturally occurring L-channel inhibitor in cardiomyocytes: relevance to human heart failure. Am J Physiol Heart Circ Physiol. 2003;285:H442-8.

Guanylin

Lessa LM, Carraro-Lacroix LR, Crajoinas RO, et al. Mechanisms underlying the inhibitory effects of uroguanylin on NHE3 transport activity in renal proximal tubule. Am J Physiol Renal Physiol. 2012;303:F1399-408.

PPP1R14A

Li Z, Yu L, Zhang Y, Gao J, et al. Identification of human, mouse and rat PPP1R14A, protein phosphatase-1 inhibitor subunit 14A, & mapping human PPP1R14A to chromosome 19q13.13-q13.2. Mol Biol Rep. 2001;28:91-101.

ATOX1

Zhang S, Liu H, Amarsingh GV, et al. Diabetic cardiomyopathy is associated with defective myocellular copper regulation and both defects are rectified by divalent copper chelation. Cardiovasc Diabetol. 2014 Jun 14;13:100. doi: 10.1186/1475-2840-13-100.

PAPP-A

Donegan D, Bale LK, Conover CA. PAPP-A in normal human mesangial cells: effect of inflammation and factors related to diabetic nephropathy. J Endocrinol. 2016;231:71-80.

Galectin-4

Perez Bay AE, Schreiner R, Benedicto I, Rodriguez-Boulan EJ. Galectin-4-mediated transcytosis of transferrin receptor. J Cell Sci. 2014;127:4457-69.

FAM3D

Rhee J, Freeman R, Roh K, et al. Cardioprotective and anti-inflammatory effects of FAM3D in myocardial ischemia-reperfusion injury. Circ Res. 2023;133:651-653.

OTUD7B

Du BB, Zhang JL, Kong LY, et al. Ovarian tumor domain-containing 7b attenuates pathological cardiac hypertrophy by inhibiting ubiquitination and degradation of Krüppel-like factor 4. J Am Heart Assoc. 2023 Dec 19;12(24):e029745. doi: 10.1161/JAHA.123.029745.

SDF-1

Cheng M, Chen C, Yu K, et al. Ablation of CXCR4 expression in cardiomyocytes exacerbates isoproterenol-induced cell death and heart failure. Int J Mol Med. 2023 Feb;51(2):13.

LaRocca TJ, Altman P, Jarrah AA, et al. CXCR4 cardiac specific knockout mice develop a progressive cardiomyopathy. .Int J Mol Sci. 2019 May 8;20(9):2267. doi: 10.3390/ijms20092267.

UBE2L6
Afsar M, Liu G, Jia L, et al. Cryo-EM structures of Uba7 reveal the molecular basis for ISG15 activation and E1-E2 thioester transfer. Nat Commun. 2023 Aug 8;14(1):4786. doi: 10.1038/s41467-023-39780-z.

PSMD9
Raffeiner M, Zhu S, González-Fuente M, Üstün S. Interplay between autophagy and proteasome during protein turnover. Trends Plant Sci. 2023;28:698-714.

ANGPTL4
Zhan W, Tian W, Zhang W, Tian H, Sun T. ANGPTL4 attenuates palmitic acid-induced endothelial cell injury by increasing autophagy. Cell Signal. 2022 Oct;98:110410. doi: 10.1016/j.cellsig.2022.110410

EpCAM
Trzpis M, McLaughlin PM, van Goor H, Brinker MG, van Dam GM, de Leij LM, Popa ER, Harmsen MC. Expression of EpCAM is up-regulated during regeneration of renal epithelia. J Pathol. 2008;216:201-8.

TNFSF14
Wu Y, Zhan S, Chen L, et al. TNFSF14/LIGHT promotes cardiac fibrosis and atrial fibrillation vulnerability via PI3Kgamma/SGK1 pathway-dependent M2 macrophage polarisation. .J Transl Med. 2023 Aug 14;21(1):544. doi: 10.1186/s12967-023-04381-3.

Li Y, Tang M, Han B, et al. Tumor necrosis factor superfamily 14 is critical for the development of renal fibrosis. Aging (Albany NY). 2020;12:25469-25486.

Yang Y, Meng L, Wu S, et al. LIGHT deficiency aggravates cisplatin-induced acute kidney injury by upregulating mitochondrial apoptosis. Int Immunopharmacol. 2020 Dec;89(Pt A):106999. doi: 10.1016/j.intimp.2020.106999.

Calcitonin (α–CRGP)
Hemmingsen C. Regulation of renal calbindin-D28K. Pharmacol Toxicol. 2000:87 Suppl 3:5-30.

Franco-Cereceda A, Gennari C, Nami R, et al. Cardiovascular effects of calcitonin gene-related peptides I and II in man. Circ Res. 1987;60:393-7.

Elafin
Ohta K, Nakajima T, Cheah AY, et al. Elafin-overexpressing mice have improved cardiac function after myocardial infarction. Am J Physiol Heart Circ Physiol. 2004;287:H286-92.

Prorelaxin H2 (RLN2)
Squecco R, Sassoli C, Garella R, et al. Inhibitory effects of relaxin on cardiac fibroblast-to-myofibroblast transition: an electrophysiological study. Exp Physiol. 2015;100:652-66.

Dschietzig T, Alexiou K, Kinkel HT, Baumann G, Matschke K, Stangl K. The positive inotropic effect of relaxin-2 in human atrial myocardium is preserved in end-stage heart failure: role of G(i)-phosphoinositide-3 kinase signaling. J Card Fail. 2011;17:158-66.

Hewitson TD, Ho WY, Samuel CS. Antifibrotic properties of relaxin: in vivo mechanism of action in experimental renal tubulointerstitial fibrosis. Endocrinology. 2010;151:4938-48.

CELSR2
Shima Y, Copeland NG, Gilbert DJ, et al. Differential expression of the seven-pass transmembrane cadherin genes Celsr1-3 and distribution of the Celsr2 protein during mouse development. Dev Dyn. 2002;223:321-32.

ICAM4
Lee G, Lo A, Short SA, et al. Targeted gene deletion demonstrates that the cell adhesion molecule ICAM-4 is critical for erythroblastic island formation. Blood. 2006;108:2064-71.

SLURP1
Swamynathan S, Tiwari A, Loughner CL, et al. The secreted Ly6/uPAR-related protein-1 suppresses neutrophil binding, chemotaxis, and transmigration through human umbilical vein endothelial cells. Sci Rep. 2019 Apr 11;9(1):5898. doi: 10.1038/s41598-019-42437-x.

Proenkephalin-A
Takasaki Y, Wolff RA, Chien GL, van Winkle DM. Met5-enkephalin protects isolated adult rabbit cardiomyocytes via delta-opioid receptors. Am J Physiol. 1999;277:H2442-50.

Liu C, Liu X, He Z, et al. Proenkephalin-A secreted by renal proximal tubules functions as a brake in kidney regeneration.. Nat Commun. 2023 Nov 7;14(1):7167. doi: 10.1038/s41467-023-42929-5.

CYB5R2
Taketani S, Ishigaki M, Mizutani A, et al.. Heme synthase (ferrochelatase) catalyzes the removal of iron from heme and demetalation of metalloporphyrins. Biochemistry. 2007;46:15054-61.

Yang MX, Cederbaum AI. Interaction of ferric complexes with NADH-cytochrome b5 reductase and cytochrome b5: lipid peroxidation, H2O2 generation, and ferric reduction. Arch Biochem Biophys. 1996;331:69-78.

JAM-C
Arcangeli ML, Frontera V, Bardin F, et al. JAM-B regulates maintenance of hematopoietic stem cells in the bone marrow. Blood. 2011;118:4609-19.

IGFBP4
Xue Y, Yan Y, Gong H, et al.. Insulin-like growth factor binding protein 4 enhances cardiomyocytes induction in murine-induced pluripotent stem cells. J Cell Biochem. 2014;115:1495-504.

Barile L, Cervio E, Lionetti V, et al. Cardioprotection by cardiac progenitor cell-secreted exosomes: role of pregnancy-associated plasma protein-A. Cardiovasc Res. 2018;114:992-1005.

CDNF
Liu H, Yu C, Yu H, et al. Cerebral dopamine neurotrophic factor protects H9c2 cardiomyocytes from apoptosis. Herz. 2018;43:346-351.

GM2A
Mundel TM, Heid HW, Mahuran DJ, Kriz W, Mundel P. Ganglioside GM2-activator protein and vesicular transport in collecting duct intercalated cells. J Am Soc Nephrol. 1999;10:435-43.

SCPEP1
Wan X, Li X, Bo H, et al.. All-trans retinoic acid protects renal tubular epithelial cells against hypoxia induced injury in vitro. Transplant Proc. 2013;45:497-502.

Xu Y, Gao AM, Ji LJ, et al.. All-trans retinoic acid attenuates hypoxia-induced injury in NRK52E cells via inhibiting NF-x03BA;B/VEGF and TGF-β2/VEGF pathway. Cell Physiol Biochem. 2016;38:229-36.